Biochimica et Biophysica Acta, 638 (1981) 173–177
Elsevier/North-Holland Biomedical Press

BBA Report

BBA 41349

MÖSSBAUER SPECTROSCOPY STUDIES OF PHOTOSYNTHETIC REACTION CENTERS FROM *RHODOPSEUDOMONAS SPHAEROIDES* R-26

BRIAN BOSO [a], PETER DEBRUNNER [a], MELVIN Y. OKAMURA [b] and GEORGE FEHER [b]

[a] *Department of Physics, University of Illinois at Urbana-Champaign, 1110 West Green Street, Urbana, IL 61801 and* [b] *Department of Physics, University of California, San Diego, CA 92093 (U.S.A.)*

(Received June 15th, 1981)

Key words: Reaction center; Mössbauer spectroscopy; Bacterial photosynthesis; Crystal field model

^{57}Fe Mössbauer spectroscopy measurements on reaction centers differing in ubiquinone content, detergent, oxidation state, or the presence of *o*-phenanthroline all show a single quadrupole doublet of similar splitting (ΔE_Q), center shift (δ) and temperature dependence. The results are indicative of high-spin Fe^{2+} with an approximately invariant first coordination sphere. A crystal field model with strong electron delocalization can account for the temperature dependence of ΔE_Q, but further data are needed to achieve a unique parameterization.

The reaction centers from photosynthetic bacteria contain an iron atom in the quinone (Q_I-Q_{II}) acceptor region [1]. It has been postulated that this iron facilitates electron transfer from the primary (Q_I) to the secondary (Q_{II}) quinone [2,3], but such a function has not been established beyond doubt [4]. The iron manifests itself mainly through the extreme broadening of the EPR spectrum of the semiquinone state of the acceptor [2,5,6], but also affects other EPR centers in the reaction center [7–9]. Striking analogies to the bacterial reaction centers have recently been reported in Photosystem II of green plants, where a 52 G exchange splitting in the EPR signal of the intermediate acceptor could be correlated with the presence of iron and plastoquinone [10]. It is of considerable interest, therefore, to characterize the electronic state of the iron in the well defined bacterial reaction centers.

Earlier Mössbauer spectroscopy measurements [11] showed that the iron is in the high-spin Fe^{2+} state ($S = 2$) in native as well as chemically reduced reaction centers. Magnetic susceptibility [12] and extended X-ray absorption fine structure [13] experiments further characterized the iron site. Here we report Mössbauer spectroscopy data on frozen aqueous solutions of six different preparations of reaction centers isolated from the photosynthetic bacterium *Rhodopseudomonas sphaeroides* R-26. The samples differed in ubiquinone content (0.10, 1.02, 2.06 Q per reaction center), detergent (LDAO or Triton X-100), oxidation state (native or dithionite-reduced in Triton X-100), or the presence of the electron-transfer inhibitor *o*-phenanthroline.

The sample preparation followed earlier procedures [1,2] as described in Ref. 12, apart from the fact that the bacteria were grown in a ^{57}Fe-enriched medium. Triton X-100 was substituted for LDAO in two samples, one of which was reduced with dithionite. (LDAO reacts with dithionite, while Triton X-100 does not.) The extent of reduction was 99.5% as determined by EPR spectroscopy according to Ref. 12. All samples were kept at 77 K until ready to run. Final sample details are listed in Table I.

Mössbauer spectra were recorded with a constant acceleration spectrometer. Two variable temperature cryostats were used, one of which was equipped with

Abbreviation: LDAO, lauryldimethylamine *N*-oxide.

TABLE I

^{57}Fe REACTION CENTER PREPARATIONS AND THEIR MÖSSBAUER PARAMETERS AT 4.2 K, $H = 0$

^{57}Fe added was 91.4% isotopically enriched. Estimated final isotopic enrichment in the sample is 78%. $A_1(A_2)$ is the area of the lower (higher) energy line.

Sample	Q/reaction center (±0.05)	A_{800}^{1cm} (±5)	Volume (ml)	Detergent	State	ΔE_Q (mm/s) (±0.002)	δ (mm/s) (±0.005)	Γ_m (mm/s) (±0.01)	A_1/A_2 (±0.02)
1	0.10	164	0.35	LDAO	oxidized	2.286	1.167	0.430	1.08
2	1.02	302	0.57	LDAO	oxidized	2.217	1.169	0.353	1.04
3 [a]	1.04	300	0.59	LDAO	oxidized	2.220	1.178	0.415	1.08
4	2.06	316	0.56	LDAO	oxidized	2.172	1.179	0.345	1.04
5	1.02	294	0.60	Triton	oxidized	2.159	1.164	0.310	1.03
6	1.02	294	0.31	Triton	reduced [b]	2.281	1.192 [c]	0.592 [c]	1.12

[a] *o*-Phenanthroline was added to this sample.
[b] Measured by EPR.
[c] These values are artificially high due to the presence of a magnetic interaction.

a superconducting magnet. Doppler shifts were calibrated periodically with an iron foil, and all velocities are given relative to the center of gravity of metallic iron at 300 K.

The zero-field spectra were analyzed using least-squares fits with two Lorentzians. Table I lists the parameters deduced from the 4.2 K data, specifically, the quadrupole splitting ΔE_Q, the center shift δ, the full width at half maximum Γ_m, and the ratio of the areas A_1 and A_2 of the lines at lower and higher energy, respectively. Figs. 1 and 2 show the temperature dependence of δ and ΔE_Q for the various samples.

Inspection of these results and comparison with other Mössbauer spectroscopy data [14–16] suggest a number of conclusions:

(i) The spectra indicate a high degree of purity of all six samples. Apart from a single quadrupole doublet no other iron species is detectable, and the ratio A_1/A_2 of the areas of the two quadrupole lines is close to unity, the value expected for a pure, randomly oriented sample with an isotropic recoilless fraction.

(ii) The linewidths Γ_m are comparable with those of other high-spin Fe^{2+} proteins ($\Gamma_m = 0.34$ mm/s for myoglobin [17] and 0.37 mm/s for horseradish peroxidase [18]). While Γ_m exceeds the minimum instrumental linewidth, $\Gamma \approx 0.24$ mm/s, in all cases and thus indicates some inhomogeneity of the iron sites, it is significant that the smallest linewidths are displayed by samples 2, 4 and 5, in which the tightly bound ubiquinone Q_I has not been removed, and no inhibitor has been added. The reduced sample 6 shows nonLorentzian lines at low temperatures due to magnetic interaction with the semiquinone free radical $Q_I^{\cdot-}$, and thus the value of Γ_m listed in Table I is not representative of the homogeneity of the iron sites.

(iii) The Mössbauer spectral parameters δ and ΔE_Q of the six samples are surprisingly similar, and little difference is discernible in their temperature dependence (Figs. 1 and 2). The center shift δ is the sum of two terms, one being the second-order Doppler shift, a purely dynamic effect that accounts for the temperature dependence, and the other arising from the electric monopole interaction of the s-electrons with the ^{57}Fe nucleus. The latter depends strongly on the shielding of the s-shells by the valence electrons and varies substantially with the ionic or covalent character of the bonds. While Mössbauer spectroscopy does not allow one to deduce the number and type of ligands coordinated to the iron, some broad, empirical correlations have nevertheless been established [14]. The center shift $1.164 \leqslant \delta \leqslant 1.192$ mm/s of the six reaction center samples at 4.2 K (Table I) lies outside the range of values reported for (a) 4-coordinated Fe^{2+} complexes ($\delta = 0.64 \pm 0.06$ mm/s for iron-sulfur proteins and model compounds [19], and 0.9 ± 0.1 mm/s for (pseudo) halides [14]), (b) 5- and 6-coordinated heme complexes ($\delta = 0.9 \pm 0.1$ mm/s

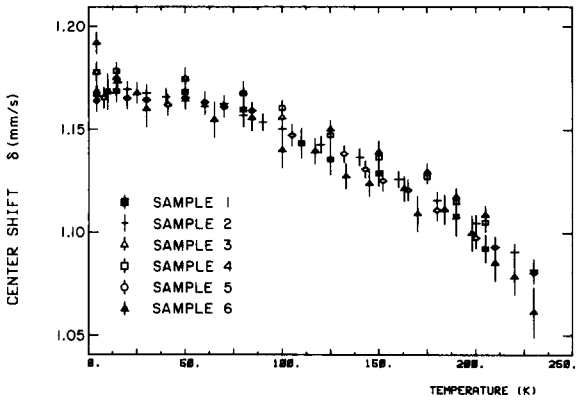

Fig. 1. Center shifts δ vs. temperature for all six samples. All values are relative to metallic iron at 300 K. (See Table I for details.)

[20,21]) and (c) complexes with six oxygen atoms coordinated to the iron (δ = 1.35 ± 0.1 mm/s [14]). Center shifts of about 1.2 mm/s are frequently found,

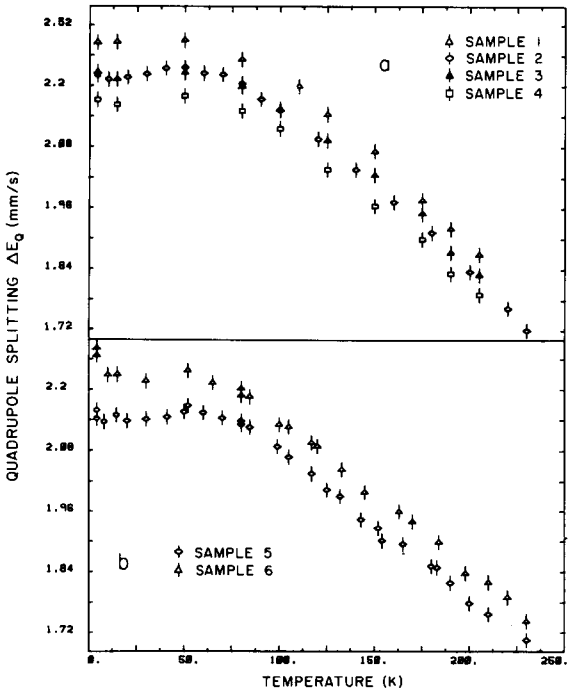

Fig. 2. Quadrupole splittings ΔE_Q vs. temperature for (a) native reaction centers in LDAO with 0.10Q (ϕ), 1.02Q (ϕ), 2.06Q (ϕ), and 1.04Q with *o*-phenanthroline added (ϕ), and (b) native reaction centers in Triton X-100 (ϕ) and dithionite-reduced reaction centers in Triton X-100 (ϕ). The samples are characterized in Table I.

however, in high-spin Fe^{2+} complexes of the type $Fe^{2+}(N...)_4X_2$, where N... may be pyridine or a bidentate ligand like *o*-phenanthroline and X is a (pseudo) halide [14]. These empirical rules therefore suggest mixed coordination of the iron to nitrogen and presumably oxygen. The narrow range of δ values found in the six reaction center samples gives no evidence for substantial changes in the first coordination sphere of the iron *.

(iv) The temperature dependence of ΔE_Q for the six samples (Fig. 2) is almost identical. In high-spin Fe^{2+} compounds this variation typically arises from the thermal population of excited orbital states [22]. For many inorganic Fe^{2+} complexes a crystal field model provides an adequate description of the electric and magnetic properties in terms of three adjustable parameters, an axial and a rhombic potential term, B_2^0 and B_2^2, and the spin-orbit coupling constant, λ [22,23]. Similar attempts for organic Fe^{2+} compounds have been less successful, presumably because organic ligands may engage in mixed σ- and π-bonds that lead to electronic states of low symmetry. High-spin Fe^{2+} heme proteins, for which up to seven parameters [24] have been used to reproduce the electric and magnetic properties, are typical.

With the above reservations in mind we attempted to fit the quadrupole splitting of reaction centers using a model calculation based on the $^5T_{2g}$ manifold, $|xy\rangle$, $|yz\rangle$ and $|xz\rangle$, of the 3d-electrons, but ignoring lattice and p-electron contributions [22,25]. The wave functions and energies are found by diagonalizing the Hamiltonian [22]:

$$H = B_2^0(3z^2 - r^2) + 3B_2^2(x^2 - y^2) + \alpha^2\lambda_0(L \cdot S) \qquad (1)$$

Here the free-ion spin-orbit coupling constant, $\lambda_0 = -144$ K, has been multiplied by the covalency factor $\alpha^2 < 1$ to account for delocalization of the 3d-orbi-

* The sensitivity of δ and ΔE_Q to changes in the first coordination sphere can be illustrated by data on high-spin Fe^{2+} porphyrins. Collman et al. [26] report δ = 0.89 mm/s, ΔE_Q = 2.38 mm/s and δ = 0.98 mm/s, ΔE_Q = 2.13 mm/s for the 'tailed picket fence' porphyrins $FePiv_3$(5ClmP)Por and $FePiv_3$(4ClmP)Por, respectively. The changes in δ and ΔE_Q are larger than those between reaction centers with 0, 1 or 2 Q/reaction center in spite of the fact that only the length of the chain linking the axial nitrogen base to the porphyrin ring has been changed.

tals. The energy levels obtained from Eqn. 1 are depicted in the inset of Fig. 3 *. Following Refs. 22 and 25 the quadrupole splitting is given by:

$$\Delta E_Q(T) = (2/7)e^2Q\langle r^{-3}\rangle_{\text{eff}}\alpha^2F(T) \quad (2)$$

$$\cong (4.0\ \text{mm/s})\,\alpha^2F(T) \quad (3)$$

with

$$F(T) = \{\langle l_{zz}\rangle_T^2 + 1/3(\langle l_{xx}\rangle_T - \langle l_{yy}\rangle_T)^2\}^{1/2} \quad (4)$$

Here $Q \simeq 0.21$ barn is the nuclear quadrupole moment, $\langle r^{-3}\rangle_{\text{eff}} = 2.23 \cdot 10^{25}\ \text{cm}^{-3} = 3.3$ a.u. is an effective inverse cube radius of the 3d-electrons, and $\langle l_{kk}\rangle_T$ is a thermal average of the quadrupole tensor $\langle l_{kk}\rangle$ calculated from the eigenstates and eigenvalues of Eqn. 1.

No acceptable fit of $\Delta E_Q(T)$ is found for any combination of the three parameters B_2^0, B_2^2 and α^2 of this model. With an additional parameter, however, the curves in Fig. 3 are obtained. Curves A and B assume a constant lattice or covalency contribution $\langle l_{zz}\rangle_L$ in addition to the temperature-dependent valence term $\langle l_{kk}\rangle_T$. Both provide acceptable fits with essentially degenerate energy eigenvalues. An extremely good fit, curve C, is obtained if different covalency factors are used to multiply the spin-orbit coupling constant λ_0 and the radial average $\langle r^{-3}\rangle$. The parameters used to calculate the three curves are listed in the inset of Fig. 3. None of these solutions agree with the parameters deduced with a similar model from the magnetic susceptibility measurements [12], which yield $D1 \approx 490$ K, $D2 \approx 810$ K and $\lambda/\lambda_0 \approx 0.50$. We conclude that a more sophisticated model is needed to fit simultaneously the magnetic and electric properties of the iron.

(v) While the six plots of ΔE_Q vs. T in Fig. 2 have the same shape and thus indicate, within experimental error, the same $F(T)$ value of Eqn. 2 for all samples, there are significant differences in magnitude. The slight increase in ΔE_Q upon reduction or with

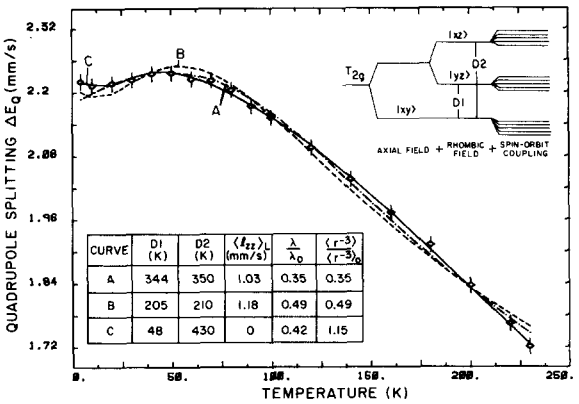

Fig. 3. Quadrupole splitting vs. temperature for native reaction centers (sample 2) with crystal field model calculations (solid and broken curves) as described in the text. The inset lists the parameters used.

decreasing number of Q/reaction center may arise from either a change in the temperature-independent lattice contribution $\langle l_{zz}\rangle_L$ or from an increase in electron density, i.e., of the factor $\langle r^{-3}\rangle_{\text{eff}}\,\alpha^2$ in Eqn. 2. The latter is consistent with the observation that in reduced reaction centers some overlap exists between the wave functions of the semiquinone and the iron as manifested by their isotropic exchange interaction. According to this view, the 3d-electrons delocalize onto the quinone(s), but the extra electron of the semiquinone in turn increases the 3d-electron density at the iron.

(vi) We have also measured Mössbauer spectra of reaction centers in magnetic fields (H) up to 4 T between 4.2 and 211 K. Fig. 4 shows the spectrum of native reaction centers (sample 5) at 211 K in a field of 3.75 T. The shape of the spectrum identifies the electric field gradient as positive, and places limits on the size of the asymmetry parameter η. The effective field (H_{eff}) acting on the iron nucleus is the sum of the applied field and an internal field, $\vec{H}_{\text{int}} = -\langle\vec{S}\rangle\tilde{A}/g_n\beta_n$. At high temperatures ($T > 150$ K) the spin expectation value $\langle\vec{S}\rangle$ is proportional to H and essentially isotropic, and if we ignore anisotropy in the magnetic hyperfine tensor $\tilde{A}$ we can approximate the effective field by $\vec{H}_{\text{eff}} = \vec{H}(1 - A\langle S\rangle/Hg_n\beta_n)$. A best fit of the spectrum then yields the curve of Fig. 4, where $\Delta E_Q = +1.76$ mm/s, $\delta = 1.06$ mm/s, $H_{\text{eff}} \approx 2.84$ T and the asymmetry parameter of the electric field gradient $\eta \approx 0.22 \pm 0.22$. Calculating

* With the substitutions $\mathcal{D} = -2/7\ \langle r^2\rangle\ B_2^0$, $\mathcal{E} = -2/7\ \langle r^2\rangle\ B_2^2$, $\lambda = \alpha^2\lambda_0$, Eqn. 1 is equivalent, within the t_{2g} manifold, to the terms $\mathcal{D}(L_z^2 - trL_z^2/5) + \mathcal{E}(L_x^2 - L_y^2) + \lambda\vec{L}\cdot\vec{S}$ of Eqn. A1 in Ref. 12. Here $\langle r^2\rangle$ is the mean square radius of the 3d-orbitals.

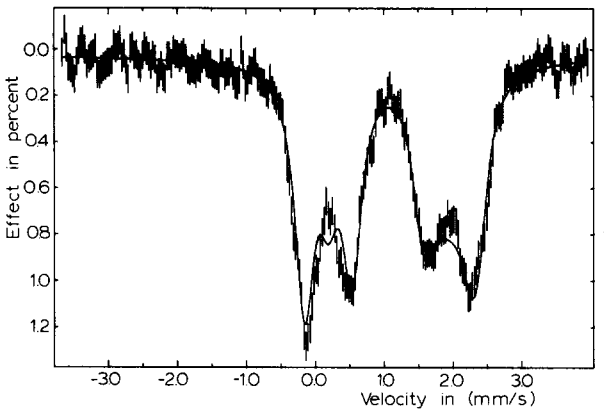

Fig. 4. Mössbauer spectrum of native reaction centers (sample 5) at 211 K in a magnetic field of 3.75 T parallel to the γ-ray beam. The solid curve is a simulation with H_{eff} = 2.84 T, ΔE_Q = +1.76 mm/s, δ = 1.09 mm/s and η = 0.22.

$\langle S \rangle$ from the results of the susceptibility measurements [12] we find an average hyperfine interaction of $A/g_n\beta_n \approx -17.5$ T.

In conclusion, Mössbauer spectroscopy shows that the iron environment in reaction centers is remarkably well defined and stable; in fact it undergoes only minor changes on removal of one or both quinones and on change of detergent or addition of *o*-phenanthroline. These results indicate that either the quinones (and *o*-phenanthroline) are not ligands of the iron, or that their removal is accompanied by a replacement with a similar ligand *. Reduction of Q_I to the semiquinone leads to a strong magnetic interaction with the iron without a comparable change in the electric interaction. Delocalization of the valence electrons is substantial and has to be taken into account explicitly in any realistic model calculation. While a four-parameter fit of the temperature dependence of the quadrupole splitting is possible, only a combined fit of the electric and magnetic hyperfine interaction can give a unique and significant set of parameters. Work along these lines is in progress.

This work was supported in part by Grants NSF PCM78-15979, DMR77-14659, PCM78-136-9 and NIH GM13191.

* See footnote, p. 175.

References

1 Feher, G. and Okamura, M.Y. (1978) in The Photosynthetic Bacteria (Clayton, R.K. and Sistrom, W.R., eds.), pp. 349–386, Plenum Press, New York
2 Okamura, M.Y., Isaacson, R. and Feher, G. (1975) Proc. Natl. Acad. Sci. U.S.A. 72, 3491–3495
3 Blankenship, R.E. and Parson, W.W. (1979) Biochim. Biophys. Acta 545, 424–444
4 Debus, R.J., Okamura, M.Y. and Feher, G. (1981) Biophys. J. 33, 19a
5 Wraight, C.A. (1977) Biochim. Biophys. Acta 459, 525–531
6 Okamura, M.Y., Isaacson, R.A. and Feher, G. (1978) Biophys. J. 21, 8a
7 Tiede, D.M., Prince, R.C., Reed, G.H. and Dutton, P.L. (1976) FEBS Lett. 65, 301–304
8 Okamura, M.Y., Isaacson, R.A. and Feher, G. (1979) Biochim. Biophys. Acta 546, 394–417
9 Bowman, M.K., Norris, J.R. and Wraight, C.A. (1979) Biophys. J. 25, 203a
10 Klimov, V.V., Dolan, E., Shaw, E.R. and Ke, B. (1980) Proc. Natl. Acad. Sci. U.S.A. 77, 7227–7231
11 Debrunner, P.G., Schulz, C.E., Feher, G. and Okamura, M.Y. (1975) Biophys. J. 15, 226a
12 Butler, W.F., Johnston, D.C., Shore, H.B., Fredkin, D.R., Okamura, M.Y. and Feher, G. (1980) Biophys. J. 32, 967–992
13 Eisenberger, P.M., Okamura, M.Y. and Feher, G. (1980) Fed. Proc. 39, 1802
14 Greenwood, N.N. and Gibb, T.C. (1971) Mössbauer Spectroscopy, Chapman and Hall, London
15 Gibb, T.C. (1976) Principles of Mössbauer Spectroscopy, Chapman and Hall, London
16 Cohen, R.L. (1976) Applications of Mössbauer Spectroscopy, vol. 1, Academic Press, New York
17 Kent, T.A., Spartalian, K., Lang, G., Yonetani, T., Reed, C.A. and Collman, J.P. (1979) Biochim. Biophys. Acta 580, 245–258
18 Champion, P.M., Chiang, R., Münck, E., Debrunner, P. and Hager, L.P. (1975) Biochemistry 14, 4159–4166
19 Debrunner, P.G., Münck, E., Que, L. and Schulz, C.E. (1977) in Iron-Sulfur Proteins (Lovenberg, W., ed.), Vol. 3, pp. 381–417, Academic Press, New York
20 Spartalian, K. and Lang, G. (1980) in Applications of Mössbauer Spectroscopy (Cohen, R.L., ed.), Vol. 2, pp. 249–279, Academic Press, New York
21 Dolphin, D., Sams, J.R., Tsin, T.B. and Wong, K.L. (1976) J. Am. Chem. Soc. 98, 6970–6975
22 Ingalls, R. (1964) Phys. Rev. 133A, 787–795
23 Varret, F. (1976) J. Phys. (Paris) C6 37, 437–456
24 Eicher, H., Bade, D. and Parak, F. (1976) J. Chem. Phys. 64, 1446–1455
25 Zimmermann, R. and Spiering, H. (1975) Phys. Status Solidi (b) 67, 487
26 Collman, J.P., Brauman, J.I., Doxsee, K.M., Halbert, T.R., Bunnenberg, E., Linder, R.E., LaMar, G.N., Del Gaudio, J., Lang, G. and Spartalian, K. (1980) J. Am. Chem. Soc. 102, 4182–4192